Electronic Supplementary Material for Chemical Communications

Supplementary Information

Fabrication of Bismuth Subcarbonate Nanotubes from Bismuth Citrate

Rong Chen,[a] Man Ho So,[a] Jun Yang,[b] Feng Deng,[b] Chi-Ming Che[a] and Hongzhe Sun *,[a]

[a] *Department of Chemistry and Open Laboratory of Chemical Biology of the Institute of Molecular Technology for Drug Discovery and Synthesis, The University of Hong Kong, Pokfulam Road, Hong Kong, China*

[b] *State Key Laboratory of Magnetic Resonance and Atomic and Molecular Physics, Wuhan Institute of Physics and Mathematics, the Chinese Academy of Sciences, Wuhan , China*

Part I.

Materials. All chemicals were purchased from Sigma-Aldrich Chemical Co. unless otherwise noted. Analytical grade organic solvents and doubly distilled deionized water were used throughout the experiments.

Instrumentation. The XRD spectrum was recorded with Philips PW1830 powder X-ray diffractometer. UV-vis spectra were taken using Varian Cary 50 spectrophotometer. TEM images of the silver nanoparticles were taken with JEOL JEM-2000 transmission electron microscopy, using an accelerating voltage of 200 kV, and were carried out on the Philips Tecnai 20 equipped with Oxford incax-sight EDX attachment using an accelerating voltage of 200 kV and Philips EM208s using an accelerating voltage of 80 kV. Solid-state ^{13}C NMR spectrum was recorded on a Varian Infinity plus-400 spectrometer equipped with a Chemagnetic 2.5 mm double resonance probe at 100.4 MHz, using CP/MAS.

Part II. Figures

Figure S1. Power XRD spectrum of $(BiO)_2CO_3$ nanotubes in the absence of CTAB.

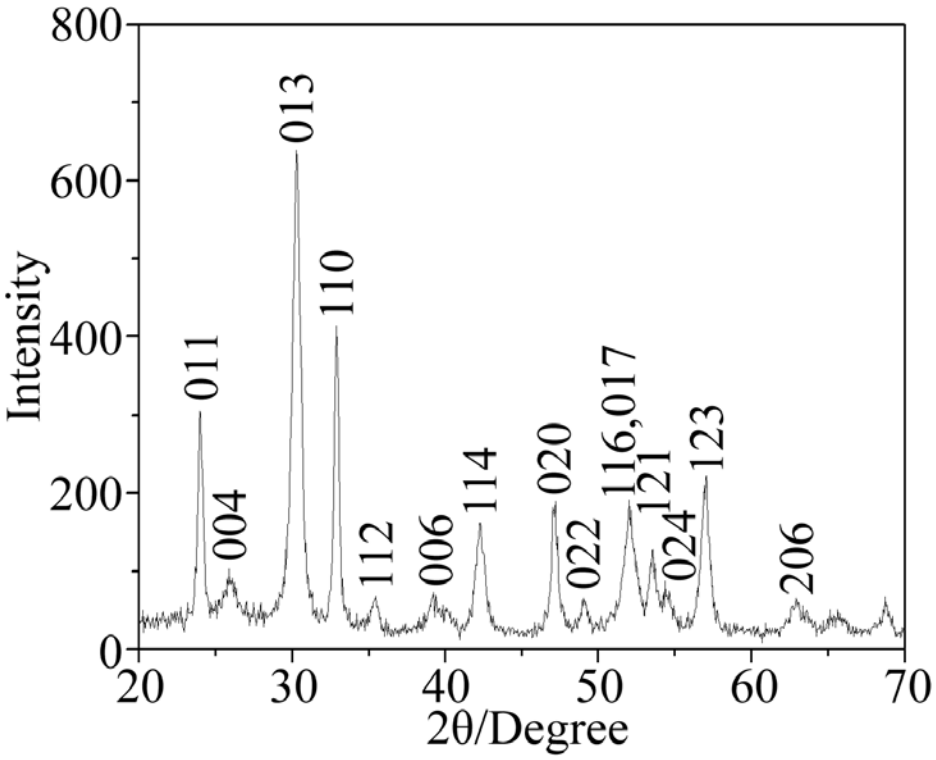

Figure S2. XPS spectrum of $(BiO)_2CO_3$ nanotubes in the absence of CTAB (a) and their high-resolution XPS spectra at carbon region (C(1*s*)) (b), oxygen region (O(1*s*) (c) and bismuth region (Bi(4*f*)) (d).

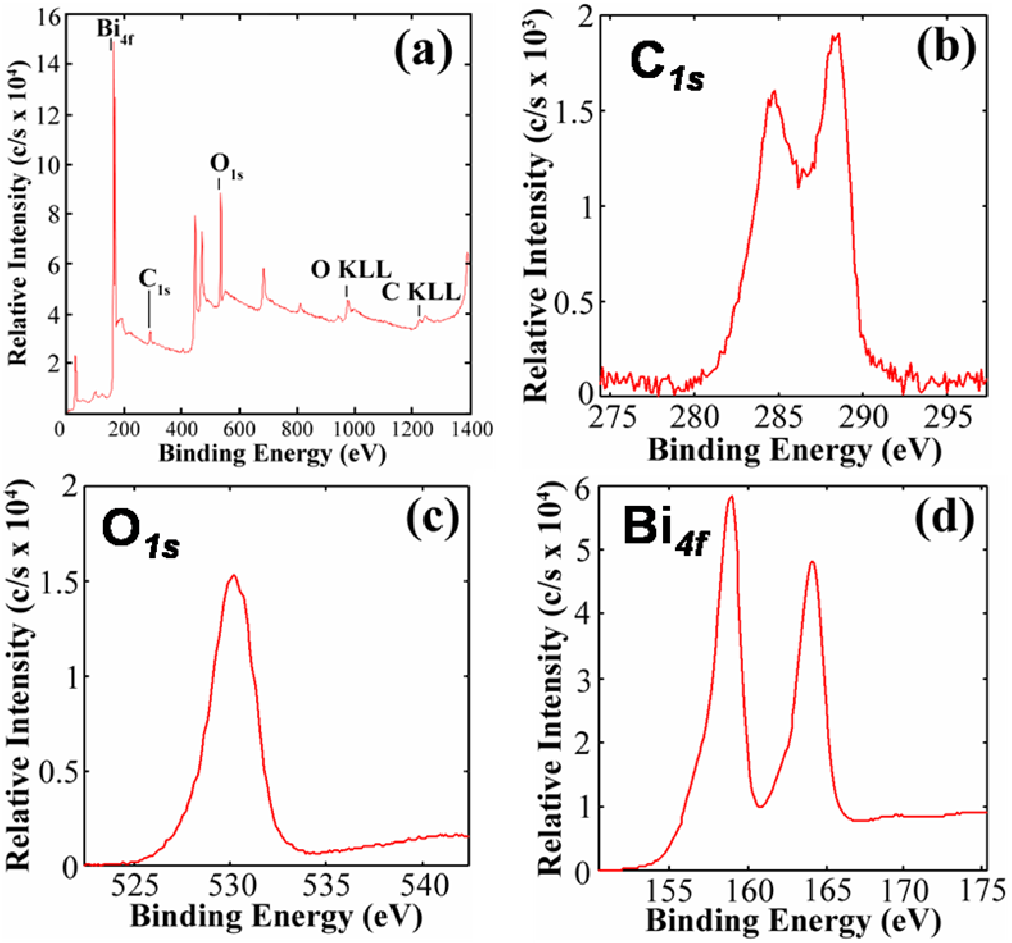

Figure S3. Scanning electron microscopy (SEM) images of the $(BiO)_2CO_3$ nanotubes (a) low magnification and (b) high magnification.

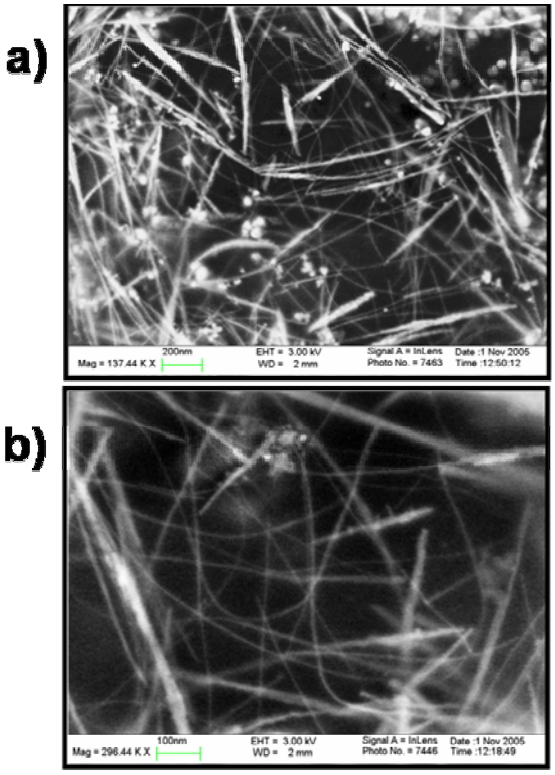

Figure S4. Diameter distribution profile of the $(BiO)_2CO_3$ nanotubes.

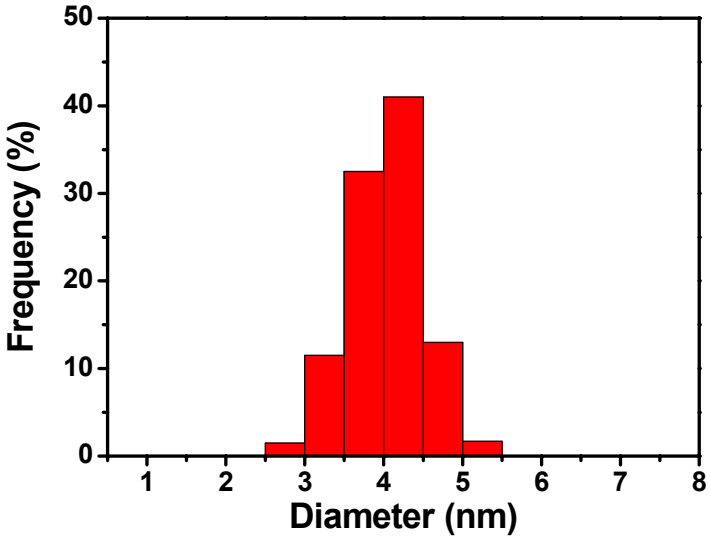

Figure S5. TEM images of $(BiO)_2CO_3$ nanoparticle line from $(BiO)_2CO_3$ nanotube after long time beam irradiation.

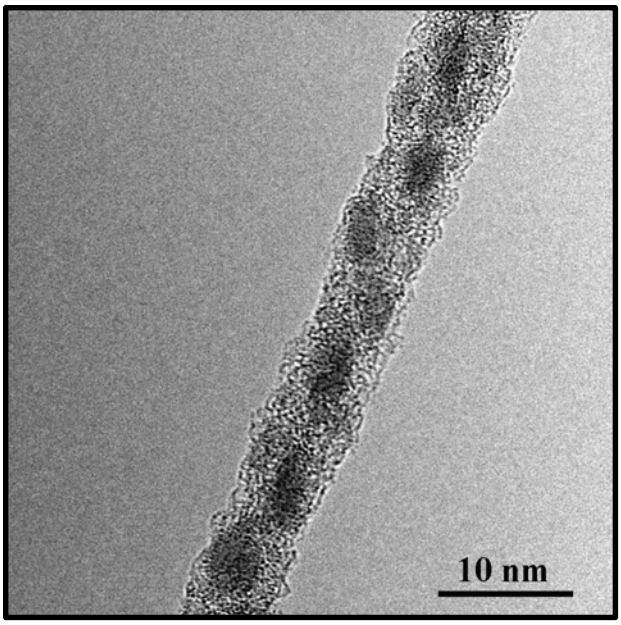

Figure S6. EDX spectrum of the $(BiO)_2CO_3$ nanotubes lying on the hole of copper grid.

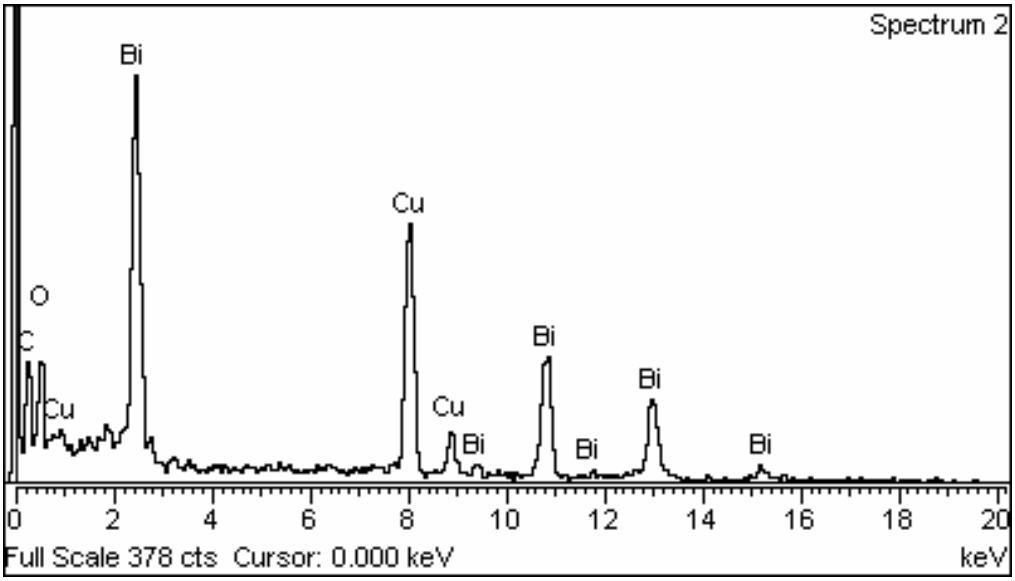

Figure S7. Solid-state ^{13}C MAS NMR spectrum of $(BiO)_2CO_3$ nanotubes. Note that the peak at 168 ppm in the ^{13}C spectrum is characteristic for bismuth bound carbonate.

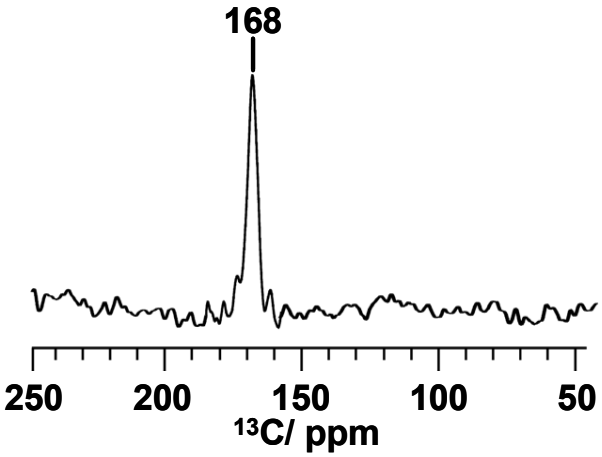

Figure S8. Schematic illustration of the function of the capping agent CTAB in the synthesis of $(BiO)_2CO_3$ nanotubes. Note that well-segregated individual $(BiO)_2CO_3$ nanotubes are formed in (c) and bundles of nanotube are formed in (e).

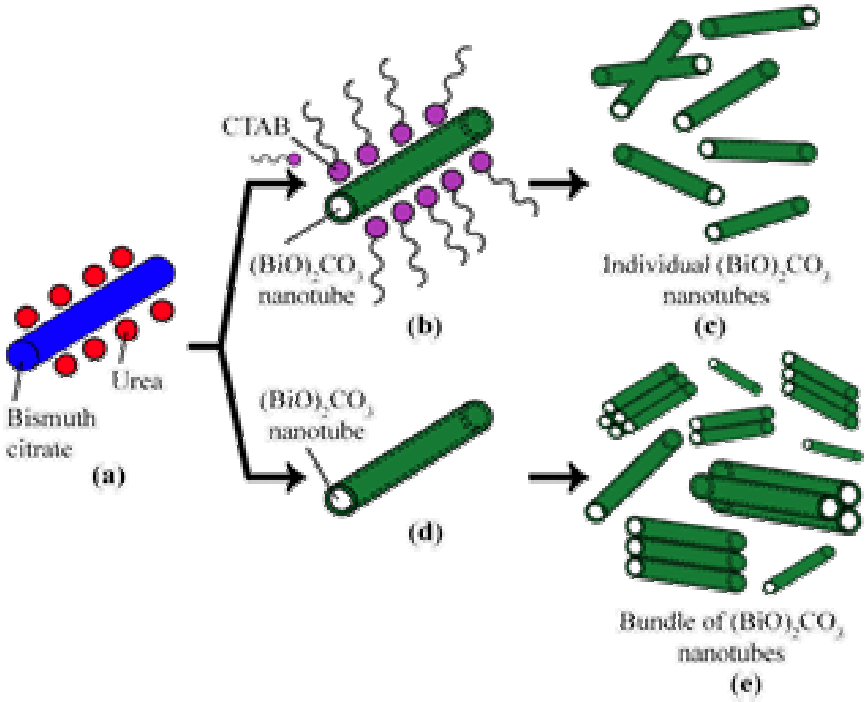

Figure S9. TEM images of selected $(BiO)_2CO_3$ nanotubes at different magnification.